Regional Climate Change Policy under Positive Feedbacks and Strategic Interactions

William Brock
Economics Department, University of Wisconsin and University of Missouri

Anastasios Xepapadeas
Department of International and European Economic Studies,
Athens University of Economics and Business

November 2, 2017

Abstract

The surface albedo feedback along with heat and moisture transport from the Equator to the Poles, are associated with polar amplification which is a well-established scientific fact. The present paper extends Brock and Xepapadeas (2017) to a non-cooperative framework with polar amplification, where regions decide emissions by maximizing own welfare. This can be regarded as a case of regional non-cooperation regarding climate change. Open loop and feedback solutions are derived and compared, in terms of temperature paths and welfare, with the cooperative solution. Carbon taxes which could bridge the gap between cooperative and non-cooperative emissions path are also derived. Finally, the framework is extended to a Ramsey set-up in which it is shown how the regional climate model can be coupled with standard optimal growth models. Numerical simulations confirm the theoretical results and provide insights about the size and the direction of deviations between the cooperative and the non-cooperative solutions.

JEL Classification: Q54 Q58

Keywords: Polar amplification, Spatial heat and moisture transport, Optimal policy, Emission taxes, Open loop, Feedback Nash Equilibrium.

1. Introduction

Understanding climate change along with its economic dimension is a complex issue that involves climate science, economics, and their interactions. The study of climate change economics is further complicated by feedbacks within the climate system. Climate feedbacks are Earth system interactions that are set in motion by the effect of a forcing factor on one part of the system. Feedbacks amplify (positive feedback) or dampen (negative feedback) the effect of a forcing factor, or cause additional change in another part of the system.

One of the well established feedbacks of the climate system is Polar or Arctic Amplification (PA or AA). Evidence indicate that the Arctic warms faster because significant positive feedbacks are taking place in the region. According to IPCC (2013, p. 396)

"Polar amplification occurs if the magnitude of zonally averaged surface temperature change at high latitudes exceeds the globally averaged temperature change, in response to climate forcings and on time scales greater than the annual cycle."

Recent studies indicate the magnitude of PA. Bekryaev et al. (2010), using an extensive data set of monthly surface air temperature, documents a high-latitude (> 60N) warming rate of 1.36C/century for 1875-2008, with the trend being almost two times stronger than the Northern Hemisphere trend of 0.79C/century.

PA which represents a feedback with geographical (i.e., spatial) origin introduces a new aspect in the study of the regional impacts of climate change. This aspect relates to the possibility that temperature changes in a location like the Arctic may generate damages to a location further away, e.g., the South. This is a kind of spatial spillover which adds another dimension to the process that associates regional damages to the global mean temperature or regional temperature, in addition to the specific characteristics of the region that is, production characteristics (e.g., agriculture vs services) or local natural characteristics (e.g., proximity to the sea and elevation).

In this context AA could be a major source of damage flows to southern regions as current research suggests.[1]

> "As emissions of greenhouse gases continue unabated, therefore, the continued amplification of Arctic warming should favour an increased occurrence of extreme events caused by prolonged weather conditions." (Francis and Skific, 2015)

[1] It should be noted that heat transfer towards the Poles could be beneficial to regions around the Equator, since it reduces temperatures and thus damages in these regions.

> "The effects of climate change on extreme weather are a topic of intense scientific interest and of vital societal impact. Some of these effects are clear – such as more severe heat waves, more frequent heavy precipitation events, and more persistent droughts – but other less direct influences are still 'up in the air'." (Francis, 2017).

The two major mechanisms associated with PA are heat transport from the Equator to the Poles and the surface albedo effect. AA apart from the potential inducement of extreme events, is also associated with another important feedback, the Arctic permafrost. According to IPCC (2013, p.9) "There is high confidence that permafrost temperatures have increased in most regions since the early 1980s. Observed warming was up to 3^0C in parts of northern Alaska (early1980s to mid-2000s) and up to 2^0C in parts of the Russian European North (1971 to 2010)." Permafrost thawing and release of greenhouse gasses (GHGs) introduces the concept of a "damage reservoir" (Brock, Engstrom and Xepapadeas, 2014) where a local change in the temperature, the AA in this case, generates global damages.[2]

Under conditions of AA due to heat transport and surface albedo feedbacks, an increase in temperature in the North will generate a "flow" of damages to the South. This can be regarded as similar to an upstream–downstream pollution problem, but the upstream problem is not generated by the actions of the upstream agent but by the collective action of agents. On the other hand, if some agents located upstream are large emitters and they realize that some of the damages will take place downstream, they might have less incentive to mitigate their emissions.

However, although PA is regarded by climate science as a near universal feature of climate model simulations of the planet's response to increasing atmospheric GHG concentrations, this feature has been largely ignored by the economics of climate science, despite evidence suggesting that AA could have important economic implications such as,[3] loss of Arctic sea ice which in turn has consequences for melting land ice; melting land ice associated with a potential meltdown of Greenland and West Antarctica ice sheets (see Lenton et al., 2008); thawing of permafrosts.

All the above are positive feedbacks which should be included in economic models. As pointed out by Dietz and Stern (2015), the science of climate change has been running years ahead of the economics of climate change. One way of

[2] "Alaska's permafrost is no longer permanent: It's thawing. The ancient carbon it is dumping into the atmosphere will make things even warmer." (New York Times, August 23, 2017). For the costs of Arctic change see for example Whiteman et al., (2013).

[3] see Brock and Xepapadeas 2017 for details.

bringing the economic of climate change closer to climate science in terms of PA, is to introduce PA induced by spatial heat transport and surface albedo effects into an economic model of climate change and to explore their impacts on the design of climate policy in the form emission paths and carbon taxes. This approach can be regarded as extending the literature on the optimal taxation of GHG emissions by accounting for the PA effect.

In a recent paper by Brock and Xepapadeas (2017) the PA effect was modelled in the context of a two-region model (Alexeev et al. 2005; Langen and Alexeev, 2007; Alexeev and Jackson 2013) with heat transport from the Equator to the Poles and potential surface albedo effects. Region or box 2 according to the climate science terminology represents the higher latitudes (30^0N to 90^0N) and region or box 1 the lower latitudes (0^0 to 30^0N). The two-box model was coupled with a simple welfare-maximization problem to derive the optimal GHG emissions path in the two regions. This solution can be regarded as the social planner's solution or the cooperative solution.

The purpose of the present paper is to extend Brock and Xepapadeas (2017) to a non-cooperative framework with PA, where regions decide emissions by maximizing own welfare. This can be regarded as the case of regional non cooperation regarding climate change. Open loop and feedback solutions are derived and compared, in terms of temperature paths and welfare, with the cooperative solution. Carbon taxes which could bridge the gap between cooperative and non-cooperative emissions path are also derived. Finally the framework is extended to a Ramsey set-up in which it is shown how the regional climate model can be coupled with standard optimal growth models.

2. Modeling Arctic Amplification

2.1. Heat Transport

In climate science terminology, models with a carbon cycle and no spatial dimension are zero-dimensional models. These models do not include spatial effects due to heat transportation across space because heat transport cannot take place across locations, since there are no distinct locations in the model. In contrast, the one- or two-dimensional energy balance climate models (EBCMs) model heat transport across latitudes or across latitudes and longitudes in continuous space (e.g. North, 1975 a,b; North et al., 1981; Wu and North, 2007). In these models the incoming absorbed radiant heat at a given latitude, in equilibrium, is

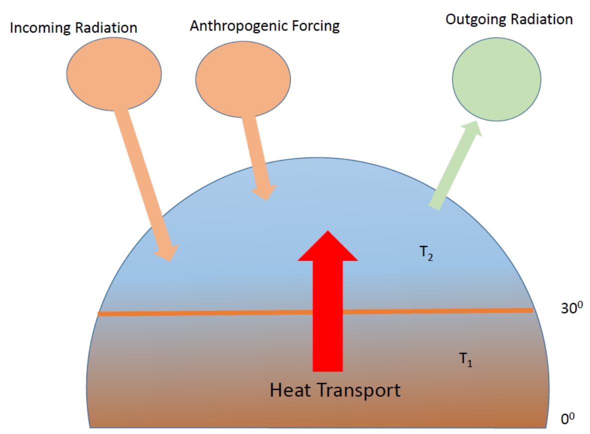

not matched by the net outgoing radiation and the difference is made by the meridional divergence of heat flux which is modelled by a diffusion term which explicitly introduces the spatial dimension stemming from the heat transport into the climate model.

EBCMs in continuous time with a spatial diffusion coefficient are quite complex to handle in economic modeling since the require dynamic optimization with partial differential equations as constraints.[4] A simpler approach is the use of the two-box energy balance model introduced by Langen and Alexeev (2007) and Alexeev and Jackson (2012). The model consists of a single hemisphere with two boxes or regions divided by the 30th latitude, which yields similar surface area of the two boxes. The two-box model of Langen and Alexeev (2007) with anthropogenic forcing is presented below.

Assuming no anthropogenic forcing, the evolution of the ocean mixed-layer temperature in each box is:

$$\dot{T}_{1T} = \frac{1}{H}\left(S_1 - A - BT_{1T} - Tr\right) \tag{1}$$

$$\dot{T}_{2T} = \frac{1}{H}\left(S_2 - A - BT_{2T} + Tr\right), \tag{2}$$

where T_{xT} , $x = 1, 2$ is the ocean mixed-layer temperatures in each region, with 1 denoting the South and 2 the North. This temperature is defined as the sum

[4] See Brock et al. (2014a), Brock and Xepapadeas (2017a).

of equilibrium, or baseline, average temperature in each box (T_{1b}, T_{2b}) when anthropogenic forcing through emissions of GHGs is zero, plus the temperature anomaly (T_1, T_2). Thus the temperature anomaly in each region is defined as $T_x = T_{xT} - T_{xb}$, $x = 1, 2$. By the definition of the regions, the baseline average yearly temperatures (T_{1b}, T_{2b}) satisfy the inequality $T_{1b} > T_{2b}$. The downwelling short wave radiation in each region is denoted by S_x, the outgoing longwave radiation by $A + BT_{xT}$, the heat transport from box 1 to box 2 by Tr, and the upper ocean layer heat capacity by H.

The meridional heat transport is defined in terms of the temperature anomaly as:

$$Tr = \bar{T}r + \gamma_1 (T_1 - T_2) + \gamma_2 T_1. \tag{3}$$

In (3) the first term, $\bar{T}r$, is the equilibrium heat transport, the second term captures the increase in transport due to increasing baroclinicity, while the third term captures the effect of an increased moisture supply and thus greater latent heat transport with increased low- to mid-latitude temperatures. To study the economics of climate change, anthropogenic forcing induced by emissions of GHGs should be introduced. The stock of GHGs created by anthropogenic emissions traps part of the outgoing longwave radiation.

Let global emissions at each date t in the two-box model be defined as the sum of emissions in box 1, $E(1,t)$, and box 2, $E(2,t)$, or $E(t) = E(1,t) + E(2,t)$. Recent results in climate science (Matthews et al., 2009; MacDougal and Friedlingstein, 2015) suggest an approximately constant transient climate response to cumulative CO_2 emissions (TCRE), λ, defined as $\lambda = \frac{\Delta T(t)}{CE(t)}$, where $CE(t)$ denotes cumulative carbon emissions up to time t and ΔT is the change in temperature during the same period. The constancy of λ suggests a linear relationship between a change of global average temperature and cumulative emissions (see also IPCC, 2013, page 1113).

Using the near proportional relationship between $CE(t)$ and $\Delta T(t)$), the anthropogenic impact on the global temperature increase can be approximated in continuous time by

$$T(t) - T(0) = \lambda \int_{s=0}^{t} E(s)\, ds, \tag{4}$$

where $CE(t) = \int_{s=0}^{t} E(s)\, ds$ denotes cumulative global carbon emissions up to time t and λ is the TCRE. Taking the time derivative of (4), we obtain

$$\dot{T}(t) = \lambda E(t). \tag{5}$$

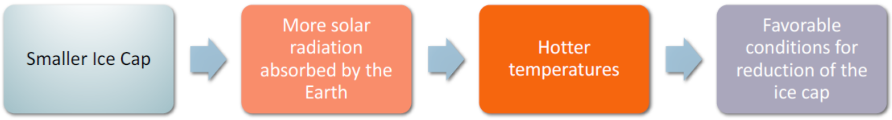

Therefore, using Langen and Alexeev (2007) parametrization and following Brock and Xepapadeas (2017) in the linearity assumption, the anthropogenic impact can be expressed in terms of the evolution of the temperature anomaly in each box as:

$$\dot{T}_1 = \frac{1}{H}\left[\left(-B-\gamma_1-\gamma_2\right)T_1+\gamma_1 T_2+\lambda E\left(t\right)\right],\ T_1\left(0\right)=0 \tag{6}$$

$$\dot{T}_2 = \frac{1}{H}\left[\left(\gamma_1+\gamma_2\right)T_1+\left(-B-\gamma_1\right)T_2+\lambda E\left(t\right)\right],\ T_2\left(0\right)=0 \tag{7}$$

$$E\left(t\right) = \left[E\left(1,t\right)+E\left(2,t\right)\right] \tag{8}$$

It is easy to show that with constant emissions $E(t)$, so a steady state exists for (6)-(8), when $\gamma_2 = 0$, the steady-state temperature anomaly between low and high latitudes is the same. On the other hand, in a steady state where $\gamma_2 > 0$, the ratio of the two anomalies is different than one. Thus the term $\gamma_2 T_1$ in (3) breaks symmetry between the two regions if $E(t)$ is constant.

2.2. Surface Albedo Feedback

The SAF mechanism suggests that initial warming in the North Pole will melt some of the Arctic's highly reflective (high albedo) snow and ice cover. This will expose darker surfaces which will absorb solar energy, leading to further warming and further retreat of snow and ice cover. This process is presented below.

As shown in Brock and Xepapadeas (2017) a simple linear SAF mechanism incorporated in this model suggests that when the SAF effect is added, region's 2 temperature will be higher and thus any damage in region 1 caused by higher temperature in region 2 will be further augmented.[5]

[5] To simplify the calibrations we are not taking into account the SAF in the rest of the paper. Brock and Xepapadeas (2017) show that the linear SAF can be included into (7) by writing the second term in the bracket as $\left(-B-\gamma_1+\alpha_2 S_2\right)T_2$, where α_2 is a co-albedo coefficient.

3. Welfare Optimization

Using the temperature dynamics (6)-(8) we study optimal paths under cooperative and noncooperative solutions. For the cooperative solution global welfare is expressed by the sum of welfare in each region:

$$\int_{t=0}^{\infty} \mathrm{e}^{-\rho t} \left[\sum_{x=1}^{x=2} v(x) L(x,t) \ln \left[y(x,t) E(x,t)^{\alpha} \mathrm{e}^{-\phi(x,T_b+T)} \right] \right] dt, \tag{9}$$

where $y(x,t) E(x,t)^{\alpha}$, $0 < \alpha < 1$, $E(x,t)$, $T_{bi}(x)$, $T_i(x,t)$ $L(x,t)$ are output per capita, fossil fuel input or emissions of GHGs, baseline temperature, temperature anomaly and fully employed population in each region x at date t, respectively. The term $\mathrm{e}^{-\phi(x,T_b+T)}$, $T_b + T = (T_{b1} + T_1, T_{b2} + T_2)$ reflects damages to output per capita in region $x = 1, 2$ from an increase in the temperature anomaly in either region, since PA in region 2 might generate damages to region 1.

By abstracting away from the problem of optimally accumulating capital inputs and other inputs, in order to focus sharply on optimal cooperative and noncooperative fossil fuel taxes, we assume that $y(x,t)$, $L(x,t)$ are exogenously given. Thus, $y(x,t)$ could be interpreted as the component of a Cobb-Douglas production function which is a composite of all other inputs along with technical change that evolves exogenously. Finally, $v(x)$ represents welfare weights associated with each region. It should be noted that this is a stylized two-region model, specially designed to focus on sharply exposing the impact of heat and moisture transport from the South towards the North Pole, on cooperative and non-cooperative climate change policies. Therefore, by necessity some important economics are left out.[6], [7]

The current value Hamiltonian for maximizing (9) subject to temperature dynamics in each region and the resource constraints is:

[6] For example, we assume fixed initial fossil fuel reserves when they are evidently not fixed (e.g., shale gas). Furthermore the model has full exhaustion of reserves. For a more realistic, but computationally intensive model, see Cai et al. (2017).

[7] We focus on the Northern Hemisphere because the geography is very different at the Southern Hemisphere, the PA is weaker there and, most importantly, most of the world's economic activity takes place North of the Equator. Evidence indicates that 88% of the global population lives in the Northern Hemisphere (http://www.radicalcartography.net/index.html?histpop).

$$
\begin{aligned}
&\mathcal{H} = \\
&\sum_{x=1}^{x=2} \left\{ v\left(x\right) L(x) \left[\alpha \ln E\left(x,t\right) - \phi\left(x, T_b + T\right)\right] - \lambda_{R_0^x} E\left(x,t\right) \right\} + \\
&\lambda_{T_1} \frac{1}{H} \left[\left(-B - \gamma_1 - \gamma_2\right) T_1 + \gamma_1 T_2 + \lambda \left[E\left(1,t\right) + E\left(2,t\right)\right]\right] + \\
&\lambda_{T_2} \frac{1}{H} \left[\left(\gamma_1 + \gamma_2\right) T_1 + \left(-B - \gamma_1\right) T_2 + \lambda \left[E\left(1,t\right) + E\left(2,t\right)\right]\right] \\
&T_b = \left(T_{b1}, T_{b2}\right) \ , \ T = \left(T_1, T_2\right),
\end{aligned}
$$

where the resource constraint on fossil fuel for each region is:

$$
\int_{t=0}^{\infty} E\left(x,t\right) dt \leq R_0\left(x\right) \ , \ x = 1, 2. \tag{10}
$$

The optimality condition for the optimal fossil fuel path is:

$$
\begin{aligned}
\frac{\alpha v\left(x\right) L\left(x\right)}{E\left(x,t\right)} &= \frac{-\lambda \left(\sum_{i=1}^{2} \lambda_{T_i}\left(t\right)\right)}{H} + \lambda_{R_0^x}\left(t\right) \quad , \text{ or} \\
E\left(x,t\right) &= \frac{-\alpha v\left(x\right) L\left(x\right) H}{\left[-\lambda \left(\sum_{i=1}^{2} \lambda_{T_i}\left(t\right)\right) + \lambda_{R_0^X}\left(t\right)\right]} \ , \ x = 1, 2.
\end{aligned}
$$

Thus, the externality tax associated with anthropogenic emissions of GHGs is determined as:

$$
\tau\left(t\right) = \frac{-\lambda \left(\sum_{i=1}^{2} \lambda_{T_i}\left(t\right)\right)}{H}. \tag{11}
$$

The externality tax is likely to increase as the cumulative carbon response parameter, λ, of Matthews et al. (2009) increases and the heat capacity H decreases.

3.1. Cross Region Damages

To explore the impact of AA on both regions in a tractable way the following assumption regrading marginal damages is made:

Assumption 1: *Define marginal damage cost of temperature increase in region* $x = 1, 2$ *by*

$$
\begin{aligned}
d_i &= \left(d_{1i}^0 + d_{2i}^0\right) + \left(d_{1i}^1 + d_{2i}^1\right) T_i(t) \\
&= \sum_{x=1}^{x=2} v(x) L(x) \frac{\partial \phi(x, T_b + T)}{\partial T_i} = d_i^0 + d_i^1 T_i(t) \ , \ i = 1, 2,
\end{aligned}
$$

where the anomaly-related damage in each box is defined as

$$
\begin{aligned}
v(1) L(1) \phi(1, T_1, T_2) &= d_{11}^0 T_1 + (1/2) d_{11}^1 (T_1)^2 \\
&\quad + d_{12}^0 T_2 + (1/2) d_{12}^1 (T_2)^2 \\
v(2) L(2) \phi(2, T_1, T_2) &= d_{21}^0 T_1 + (1/2) d_{21}^1 (T_1)^2 \\
&\quad + d_{22}^0 T_2 + (1/2) d_{22}^1 (T_2)^2 .
\end{aligned}
$$

It is assumed that d_{ij}^l, $i, j = 1, 2$, $l = 0, 1$ *are constants at all dates.*

In Assumption 1, the parameters (d_{12}, d_{21}) capture the cross effects from an increase in the temperature anomaly in one region on the damages of the other region. In particular, d_{12} captures the effects of AA in region 2 on damages in region 1.

Thus $d_1^l = d_{11}^l + d_{21}^l, l = 0, 1$ is the aggregate impact (i.e. the impact on both regions) from a temperature increase in region 1, while $d_2^l = \left(d_{12}^l + d_{22}^l\right)$ is the aggregate impact from a temperature increase in region 2. If we assume that the AA effects on region 1 are sufficiently strong, and d_{21} is negligible, then $d_2^l > d_1^l$ reflects strong PA effects. If $d_{12}^l > d_{22}^l$, the PA effects are stronger in region 1 while if $d_{12}^l < d_{22}^l$, PA effects are stronger in region 2.

The optimality conditions for the costate equations of the climate dynamics, setting without loss of generality $H = 1$, and assuming infinite reserves so that the resource shadow value, $\lambda_{R_0^x}$ is zero, imply:

$$
\begin{aligned}
\dot{\lambda}_{T_1} &= \left[\rho + (B + \gamma_1 + \gamma_2)\right] \lambda_{T_1} - (\gamma_1 + \gamma_2) \lambda_{T_2} + d_1^0 + d_1^1 T_1 && (12) \\
\dot{\lambda}_{T_2} &= -\gamma_1 \lambda_{T_1} + \left[\rho + (B + \gamma_1)\right] \lambda_{T_2} + d_2^0 + d_2^1 T_2, && (13)
\end{aligned}
$$

with steady-state values obtained by setting $\left(\dot{\lambda}_{T_1}, \dot{\lambda}_{T_2}\right) = (0, 0)$, or

$$
\lambda_{T_1}^* = \phi_1(T_1, T_2) \ , \ \lambda_{T_2}^* = \phi_2(T_1, T_2) .
$$

Then, the steady-state optimal carbon tax is defined, at $\left(\lambda_{T_1}^*, \lambda_{T_2}^*, T_1^*, T_2^*\right)$, as:

$$
\tau^* = -\lambda \left[\phi_1(T_1^*, T_2^*) + \phi_2(T_1^*, T_2^*)\right] . \qquad (14)
$$

4. Bias from Ignoring Heat Transport

We are interested in calculating the error made if the planner mistakenly ignores heat transfer Tr in computing optimal carbon taxes. To calculate this error, we compute the solution by the planner who acts as if $Tr = 0$, but $Tr \neq 0$ is present in the actual climate. In terms of the model, ignoring heat transport is equivalent to setting $\gamma_1 = \gamma_2 = 0$. We denote by $\hat{\tau} = \tau(0,0)$ the optimal carbon tax without heat transport and by $\tau(\gamma_1, \gamma_2)$ the optimal carbon tax under heat transport, i.e. $(\gamma_1, \gamma_2) \neq (0,0)$. Then the bias from ignoring heat transport can be defined as:

$$\frac{\hat{\tau}}{\tau(\gamma_1,\gamma_2)} = \frac{\tau(0,0)}{\tau(\gamma_1,\gamma_2)} \tag{15}$$

$$\tau(0,0) = \left(d_1^0 + d_2^0 + d_1^1 T_1 + d_2^1 T_2\right)(\rho + B + 2\gamma_1 + \gamma_2) \tag{16}$$

$$\begin{aligned} &\tau(\gamma_1,\gamma_2) = \\ &\big[(\rho + B + 2\gamma_1)\left(d_1^0 + d_2^0\right) \\ &+2d_2^0\gamma_2 + d_1^1(B + 2\gamma_1 + \rho)T_1 + d_2^1(B + 2(\gamma_1+\gamma_2) + \rho)T_2\big] \end{aligned} \tag{17}$$

Let $\gamma_2 \to \infty$. By applying the L' Hospital rule and reversing the ratio, we obtain

$$\frac{\tau(\gamma_1,\infty)}{\tau(0,0)} = \frac{2\left(d_2^0 + d_2^1 T_2\right)}{d_1^0 + d_2^0 + d_1^1 T_1 + d_2^1 T_2}. \tag{18}$$

The gap between the incorrect choice of "optimal" tax rate and the correct tax rate depends on the current level of the anomalies. Therefore, in order to obtain some insights about the sign and the direction of the bias we resort to numerical simulations. The values used in the simulations are described in detail in Brock and Xepapadeas (2017).

4.1. Simulation Results

We consider a case with strong AA effects (Figure 1) and a case with weak AA effects (Figure 2) according to Assumption 1.

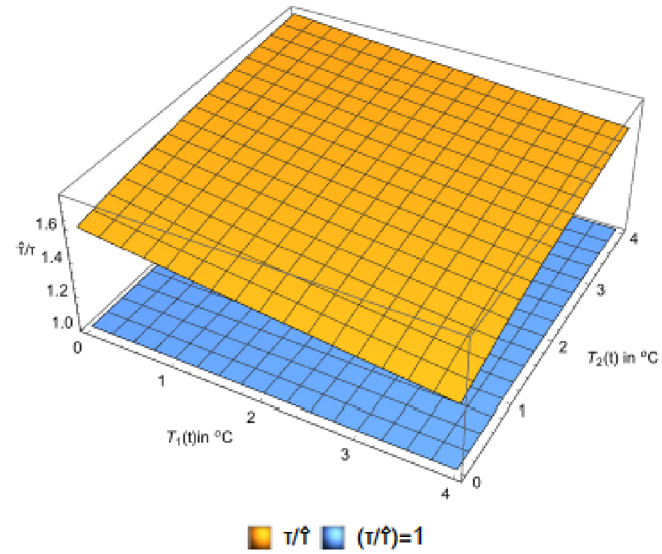

Figure 1: $d_1^0 = 0.05, d_2^0 = 0.2, d_1^1 = 0.01, d_2^1 = 0.05$, Strong AA effects

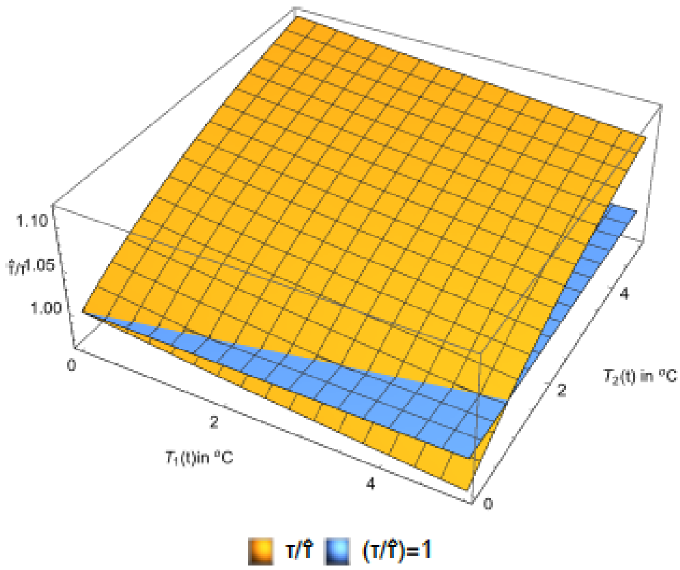

Figure 2: $d_1^0 = 0.15, d_2^0 = 0.15, d_1^1 = 0.01, d_2^1 = 0.05$, Weak AA effects

As shown in Figure 1, when the AA effects are strong the carbon tax that does not account for heat transport underestimates the optimal carbon tax. While when the AA effects are weak, the same bias occurs when the temperature anomaly in the North is high, but the result is reversed for low anomaly in the North.

To obtain insights about the optimal paths, the modified dynamic Hamiltonian system resulting from the solution of problem (9) is linearized around the saddle point steady state, and then the system of four differential equations for the temperature anomalies and the corresponding costate variables is fully solved with and without heat transport. The evolution of temperature anomalies and the expected global anomaly without heat transport effects is shown in Figure 3 when $d^l_{12} < d^l_{22}$ and in Figure 4 when $d^l_{12} > d^l_{22}$

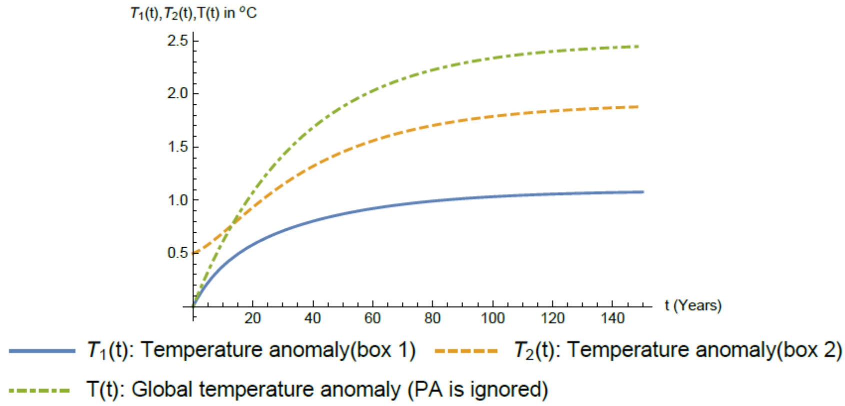

Figure 3: Regional and global temperature anomalies when $d^l_{12} < d^l_{22}$

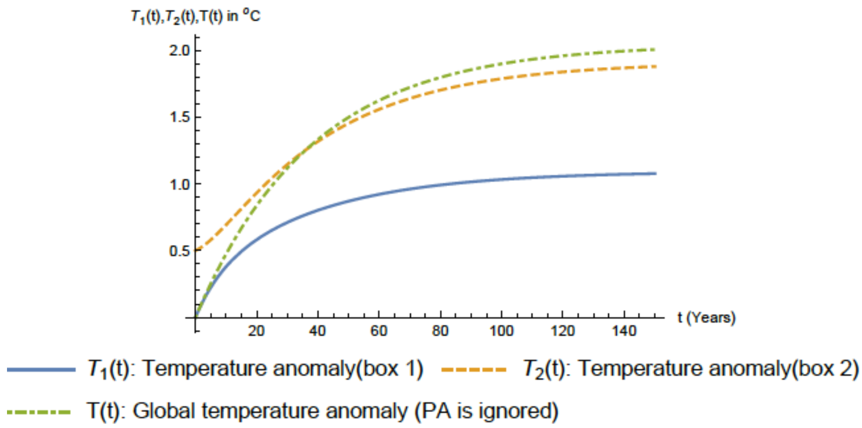

Figure 4: Regional and global temperature anomalies when $d^l_{12} > d^l_{22}$.

It is clear that in both cases ignoring heat transport will predict a path for the global anomaly which is different than the average path of the two anomalies. However, when the optimal emission paths are determined without taking into account heat transport and PA, while heat transport is actually taking place in the real climate system, then new paths for the regional anomalies will actually emerge. To determine these paths, the emission paths obtained from the optimized system, *without heat transport*, were substituted in the temperature anomalies dynamics (6)-(7), and the system was solved with the "wrong planned emissions." The results are shown in figures 5 and 6.

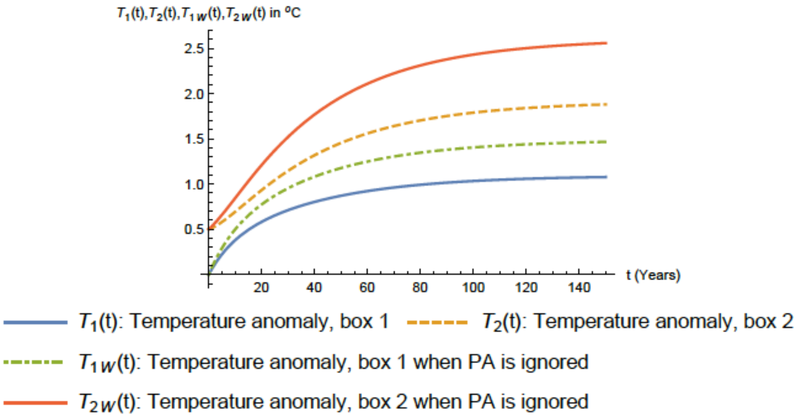

Figure 5: Evolution of temperature anomalies (T_{1W}, T_{2W}) with the wrong planned emissions relative to optimal anomalies. $d_{12}^l < d_{22}^l$

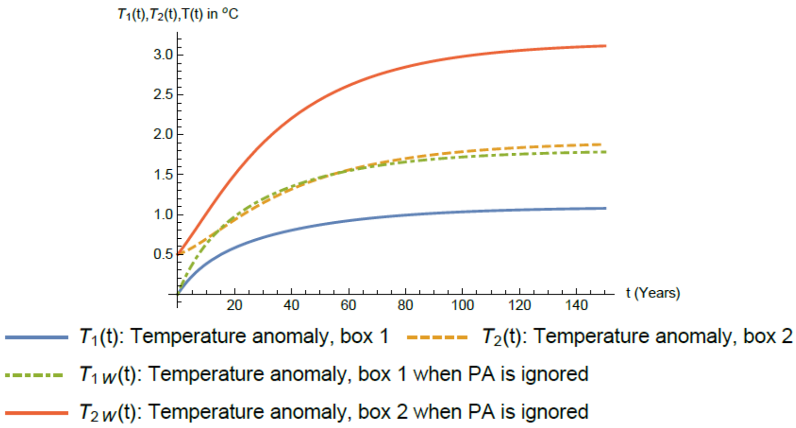

Figure 6: Evolution of temperature anomalies (T_{1W}, T_{2W}) with the wrong planned emissions relative to optimal anomalies. $d_{12}^{l} > d_{22}^{l}$

It is clear that in both cases using the “wrong planned emissions” will result in higher regional temperature anomalies relative to the optimal anomalies. This result could have significant policy implications since it implies that if heat transport is not taken into account the planned emissions will be suboptimal, and this will lead to higher than desired regional temperatures.

5. Welfare Effects

Suppose that the planner mistakenly believes that heat and moisture transport is not present, i.e. $(\gamma_1, \gamma_2) = (0, 0)$, but the true dynamics are $\gamma_1 > 0, \gamma_2 > 0$. How big is the error in welfare units and how big is the error in energy use and emissions taxes?

A proportional welfare gain for each region by accounting for PA can be defined as:

$$\psi(x) = \frac{W[x, (\gamma_1, \gamma_2) \mid (\gamma_1, \gamma_2)] - W[x, (a_1, a_2) \mid (\gamma_1, \gamma_2)]}{W[x, (a_1.a_2) \mid (\gamma_1, \gamma_2)]}, \ x = 1, 2, \tag{19}$$

as a measure of the error made by a planner who believes $(a_1.a_2)$ when the true parameters are (γ_1, γ_2).

$$\begin{aligned} & W[x, (\gamma_1, \gamma_2) \mid (\gamma_1, \gamma_2)] = \\ & \int_{t=0}^{\infty} \mathrm{e}^{-\rho t} [v(x) L(x,t) \times \\ & \ln \left[y(x,t) E(x,t \mid (\gamma_1, \gamma_2))^{\alpha} \mathrm{e}^{-\phi(x, T(\gamma_1, \gamma_2))} \right] dt \end{aligned} \tag{20}$$

$$\begin{aligned} & W[(a_1, a_2) \mid (\gamma_1, \gamma_2)] = \\ & \int_{t=0}^{\infty} \mathrm{e}^{-\rho t} [v(x) L(x,t) \times \\ & \ln \left[y(x,t) E(x,t \mid (a_1, a_2))^{\alpha} \mathrm{e}^{-\phi(x, T(a_1, a_2))} \right] dt \end{aligned} \tag{21}$$

$$(a_1, a_2) = (0, 0), \ x = 1, 2, \tag{22}$$

where $T(a_1, a_2) = (T_1(a_1, a_2), T_2(a_1, a_2))$ are the anomalies emerging from using the emissions paths derived from welfare optimization without heat transport and PA effects.

The simulation results, using a terminal time of $t = 1000$ for the numerical integration, indicate:

- $d_{12}^{l} < d_{22}^{l}$,$l = 0, 1$

$$\begin{aligned} \psi(1) &= 31.0\% \qquad (23) \\ \psi(2) &= 32.1\% \qquad (24) \end{aligned}$$

- $d_{12}^{l} > d_{22}^{l}$,$l = 0, 1$

$$\begin{aligned} \psi(1) &= 31.6\% \qquad (25) \\ \psi(2) &= 31.5\% \qquad (26) \end{aligned}$$

This result is another indication of potential suboptimal outcomes when heat transport and AA are ignored.

6. Non-Cooperative Solutions

6.1. Open Loop Nash Equilibrium (OLNE)

In a non-cooperative world, each region chooses emissions paths to maximize own welfare taking the emissions path of the other region as given, or:

$$\begin{aligned} &\max_{E(x,t)} J(x), \ x = 1, 2 \qquad (27) \\ &J(x) = \int_{t=0}^{\infty} \mathrm{e}^{-\rho t} \left[v(x) L(x,t) \ln \left[y(x,t) E(x,t)^{\alpha} \mathrm{e}^{-\phi(x, T_b + T)} \right] \right] dt \end{aligned}$$

subject to temperature dynamics and resource constraints. It is assumed that each region follows open loop strategies by committing to emission paths at the beginning of the time horizon. Then, the solution of problem (27) using the maximum principle will provide the open loop Nash equilibrium (Basar and Olsder 1995).

The current value Hamiltonian for each region is:

$$
\begin{aligned}
&\mathcal{H}_j^{OL} = \\
&v(j)\, L(j)\left[\alpha \ln E(j,t) - \phi(j, T_b + T)\right] - \lambda_{jR_0} E(j,t) + \\
&\lambda_{jT_1}^{OL} \frac{1}{H}\left[(-B-\gamma_1-\gamma_2)\, T_1 + \gamma_1 T_2 + \lambda\left[E(j,t) + \bar{E}(i,t)\right]\right] + \\
&\lambda_{jT_2}^{OL} \frac{1}{H}\left[(\gamma_1+\gamma_2)\, T_1 + (-B-\gamma_1)\, T_2 + \lambda\left[E(j,t) + \bar{E}(i,t)\right]\right] \\
&T_b = (T_{b1}, T_{b2})\ ,\ T = (T_1, T_2)\,, j \neq i,\ j = 1,2
\end{aligned}
$$

The optimality conditions for the costate equations of the climate dynamics, setting without loss of generality $H = 1$, imply:

$$
\begin{aligned}
\dot{\lambda}_{jT_1}^{OL} &= \left[\rho + (B + \gamma_1 + \gamma_2)\right] \lambda_{jT_2}^{OL} - (\gamma_1 + \gamma_2)\, \lambda_{jT_2}^{OL} + d_{j1}^0 + d_{j1}^1 T_1 \\
\dot{\lambda}_{jT_2}^{OL} &= -\gamma_1 \lambda_{jT_2}^{OL} + \left[\rho + (B + \gamma_1)\right] \lambda_{jT_2}^{OL} + d_{j2}^0 + d_{j2}^1 T_2\ ,\ j = 1,2.
\end{aligned}
$$

Given that the regions are not symmetric with respect to damages, the costates are not the same and the externality tax is different between regions. The asymmetry depends on the damage parameters. This is because in the cooperative solution the social planner takes into account damages to both regions from a change of temperature in one region, while in the non-cooperative solution each region considers damages to itself only. The structure of marginal damages in the cooperative and the noncooperative cases are shown below.

Cooperative

$\Delta T_1 : d_1^l = d_{11}^l + d_{21}^l, l = 0,1\ , \Delta T_2 : d_2^l = d_{12}^l + d_{22}^l\ ,\ l = 0,1$

Non-cooperative

Region 1: $\Delta T_1 : d_{11}^l,\ \Delta T_2 : d_{12}^l\ ,\ l = 0,1$

Region 2: $\Delta T_1 : d_{21}^l,\ \Delta T_2 : d_{22}^l\ ,\ l = 0,1$

With regional steady-state values at $\left(\dot{\lambda}_{jT_1}^{OL}, \dot{\lambda}_{jT_2}^{OL}\right) = (0,0)\,$, the steady-state optimal externality taxes at OLNE are

$$
\tau_j^* = -\lambda\left[\lambda_{jT_1}^{*OL} + \lambda_{jT_2}^{*OL}\right]. \tag{28}
$$

Solving the non-symmetric OLNE and then linearizing the Hamiltonian systems around the OLNE steady states, we obtain the OLNE paths for the temperature anomalies and the corresponding costate variables. The costate variables provide the climate externality in each region from a change in temperature in the North or the South.

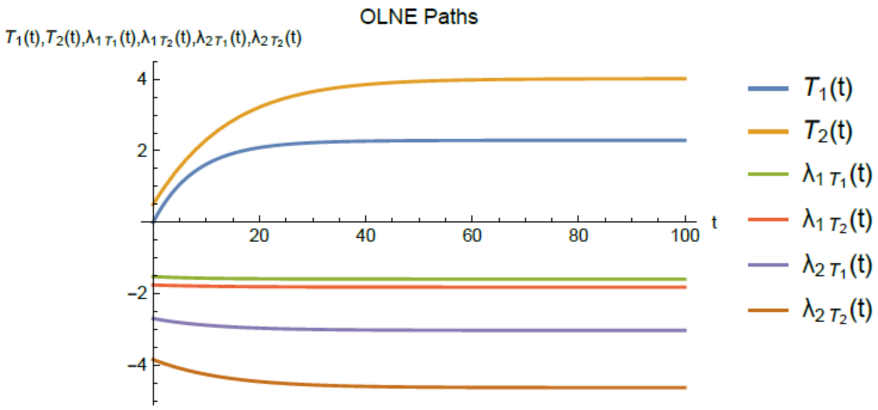

Figure 7: Temperature anomalies and costate variables at the OLNE

In figure 8 the corresponding paths are provided for the cooperative solution. As expected under OLNE the temperature anomalies are higher and the cost of climate externality lower relative to the cooperative solution.

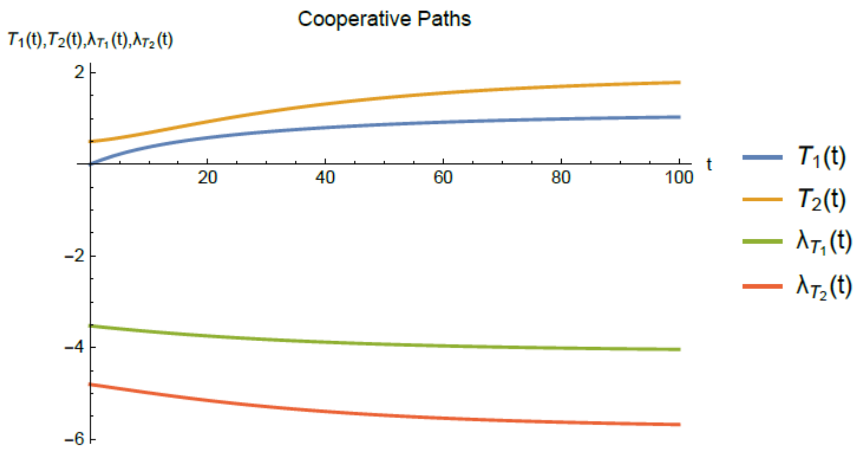

Figure 8: Temperature anomalies and costate variables at the OLNE

Table 1 below presents steady state comparisons between the cooperative solutio and OLNE.

Table 1: Steady-state comparisons

Cooperative:	$T_1 : 1.09$	$T_2 : 1.91$	$\lambda^*_{T_1} : -4.08$	$\lambda^*_{T_2} : -5.76$
OLNE $d^l_{12} < d^l_{22}$:	$T_1 : 1.85$	$T_2 : 3.23$	$\lambda^{*OL}_{1T_1} : -2.19$	$\lambda^{*OL}_{1T_2} : -2.84$
			$\lambda^{*OL}_{2T_1} : -2.73$	$\lambda^{*OL}_{2T_2} : -4.18$
OLNE $d^l_{12} > d^l_{22}$:	$T_1 : 1.90$	$T_2 : 3.34$	$\lambda^{*OL}_{1T_1} : -3.14$	$\lambda^{*OL}_{1T_2} : -4.39$
			$\lambda^{*OL}_{2T_1} : -1.82$	$\lambda^{*OL}_{2T_2} : -2.70$

Figures 7 and 8 and table 1 suggest that the optimal externality tax in each region will be lower than the cooperative tax because each region takes into account own damages. A social planner seeking to implement the cooperative tax needs to impose an additional tax in each region. This additional tax should bridge the gap between the optimal tax under full cooperation and the regional OLNE taxes, and is defined below, for the case of the steady-state tax.

$$\tau_j^{*OPT} = -\lambda \left[\lambda^*_{T_1} + \lambda^*_{T_2}\right] - \left(-\lambda \left[\lambda^{*OL}_{jT_1} + \lambda^{*OL}_{jT_2}\right]\right), \text{ Region } j = 1,2 \tag{29}$$

There are welfare gains from moving to the cooperative equilibrium which are shown in the table 2 below.

Table 2: Welfare Gains (%) from moving from OLNE to full cooperation

Region 1	$d^l_{12} < d^l_{22}$	48.9%	$d^l_{12} > d^l_{22}$	51.6%
Region 2		50.3		51.5

6.2. Feedback Nash Equilibrium (FBNE)

As it is well know the OLNE is not a strong time consistent equilibrium. To obtain a strong time consistent noncooperative equilibrium we resort to feedback strategies. It is assumed that each region follows non-symmetric time stationary feedback Nash equilibrium emission strategies of the form.

$$E_j = h_j\left(T_1, T_2\right). \tag{30}$$

Since the anomalies in both regions affect the regions welfare, it is natural to assume that each region's feedback rule will depend on both anomalies.

The obtain tractable solutions the problem is transformed into a linear quadratic (LQ) problem, by using Magill's (1977) quadratic approximation around the steady state of the OLNE. The objective function for each region in this case takes the form

$$F^j\left(q_j, u, v\right) = q_j^2 G^j_{EE} - (u, v) \begin{pmatrix} G^j_{T_1T_1} & G^j_{T_1T_2} \\ G^j_{T_2T_1} & G^j_{T_2T_2} \end{pmatrix} \begin{pmatrix} u \\ v \end{pmatrix} \tag{31}$$

$$q_j = \left(E_j - E_j^{*OL}\right), \quad (u, v) = \left(T_1 - T_1^*, T_2 - T_2^*\right), j = 1, 2, \tag{32}$$

where $G^j(E_j, T_1, T_2) = v(j) L(j) a \ln E_j - \phi_j(j, T_1, T_2)$, $j = 1, 2$ is the objective function at time t in each region with the damage function having the quadratic form defined in Assumption 1, and all derivatives evaluated at the OLNE steady state.

The HJB equation for each region becomes

$$\begin{aligned} \rho V^j(u, \upsilon) &= \max_{q_j} \left[\xi_{j1} q_j^2 - \xi_{j2} \upsilon^2 - \xi_{j3} u^2 \right. \\ &\quad + V_u^j \frac{1}{H} \left[(-B - \gamma_1 - \gamma_2) u + \gamma_1 \upsilon + \lambda \left[q_j + h_i(u, \upsilon) \right] \right] \\ &\quad \left. + V_\upsilon^j \frac{1}{H} \left[(\gamma_1 + \gamma_2) u + (-B - \gamma_1) \upsilon + \lambda \left[q_j + h_i(u, \upsilon) \right] \right] \right] \\ j, i &= 1, 2, j \neq i. \end{aligned}$$

Given the LQ structure of the problem, we consider a quadratic value function

$$V^j(u, \upsilon) = \zeta_{j1} u^2 + \zeta_{j2} \upsilon^2 + \zeta_{j3} u \upsilon \ , \ j = 1, 2.$$

6.3. Solution

The solution involves the following steps.

- Standard optimization determines emission strategies as linear feedback rules of the temperature anomalies. Since regions are asymmetric regarding damages, the two value functions have different parameters. Thus the FBNE is determined by a system of two value functions.
- Substituting the feedback rules in the HJB, and collecting terms of the same power, a nonlinear system in the six unknown parameters of the value function $(\zeta_{j1}, \zeta_{j2}, \zeta_{j3})$, $j = 1, 2$ is determined. Solution of this sytem will provide the parameters of the value function.

To obtain some insights into the solution, we calculate the parameters numerically using the same parametrization as above

The slopes of the linear feedback emission strategies in the original variables are:

$$\begin{array}{lll} d_{12}^l < d_{22}^l : & \frac{\partial E_j(T_1, T_2)}{\partial T_i} < 0 & i, j = 1, 2 \\ d_{12}^l > d_{22}^l : & \frac{\partial E_1(T_1, T_2)}{\partial T_i} < 0 & i = 1, 2 \\ & \frac{\partial E_2(T_1, T_2)}{\partial T_i} > 0 & i = 1, 2. \end{array}$$

Substituting the feedback strategies into temperature dynamics, we obtain the evolution of the temperature anomalies at the FBNE. The steady states are:

$$\begin{aligned} d^l_{12} &< d^l_{22} : T_1^{*FB} = 3.54, T_2^{*FB} = 6.20 \\ d^l_{12} &> d^l_{22} : T_1^{*FB} = 5.55, T_2^{*FB} = 9.69. \end{aligned}$$

These steady states are stabl, as shown in the phase diagrams below.

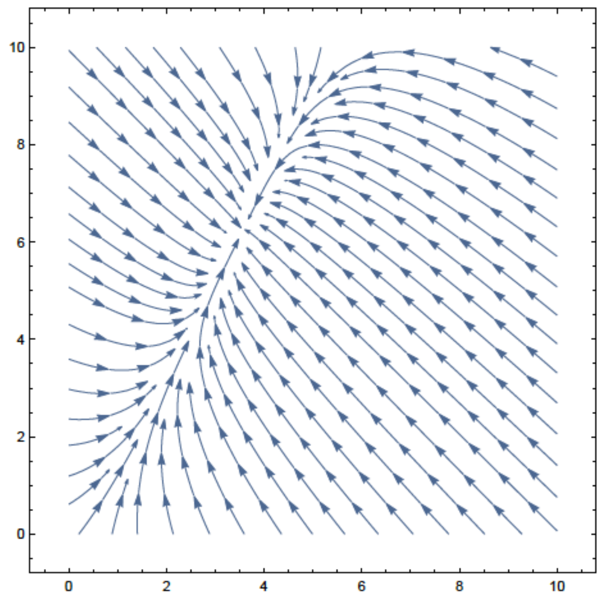

Figure 9: FBNE Steady state when $d^l_{12} < d^l_{22}$

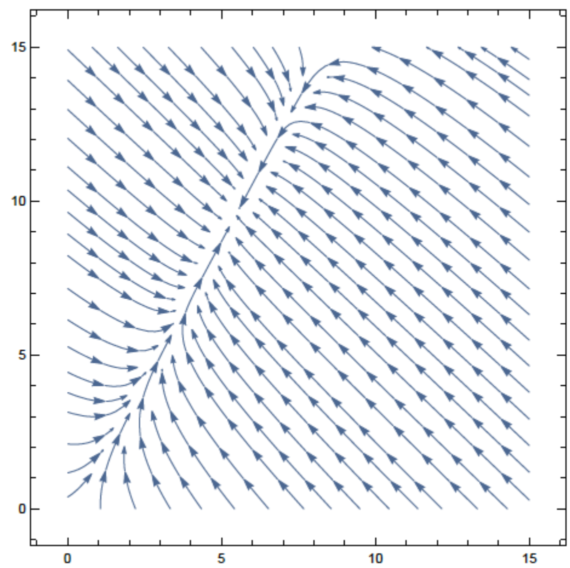

Figure 10: FBNE Steady state when $d^l_{12} > d^l_{22}$

In terms of welfare comparisons:

- When $d^l_{12} < d^l_{22}$, the SWF in region 1 is 25.6% higher than region 2.
- When $d^l_{12} > d^l_{22}$, the SWF in region 2 is 21.9% higher than region 1.

Thus the size of cross effects in terms of marginal damages play a crucial role for the equilibrium welfare in the two regions.

Table 3: Steady-state comparisons, Cooperative, OLNE, FBNE

Cooperative:	$T_1 : 1.09$	$T_2 : 1.91$	$\lambda^*_{T_1} : -4.08$	$\lambda^*_{T_2} : -5.76$
OLNE $d^l_{12} < d^l_{22}$:	$T_1 : 1.85$	$T_2 : 3.24$	$\lambda^{*OL}_{1T_1} : -2.19$	$\lambda^{*OL}_{1T_2} : -2.84$
			$\lambda^{*OL}_{2T_1} : -2.73$	$\lambda^{*OL}_{2T_2} : -4.18$
OLNE $d^l_{12} > d^l_{22}$:	$T_1 : 1.90$	$T_2 : 3.33$	$\lambda^{*OL}_{1T_1} : -3.14$	$\lambda^{*OL}_{1T_2} : -4.39$
			$\lambda^{*OL}_{2T_1} : -1.82$	$\lambda^{*OL}_{2T_2} : -2.70$
FBNE $d^l_{12} < d^l_{22}$:	$T_1 : 3.54$	$T_2 : 6.20$	$V^{*FB}_{1T_1} : -0.027$	$V^{*FB}_{1T_2} : -0.141$
			$V^{*FB}_{2T_1} : -0.173$	$V^{*FB}_{2T_2} : -0.597$
FBNE $d^l_{12} > d^l_{22}$:	$T_1 : 5.55$	$T_2 : 9.69$	$\lambda^{*OL}_{1T_1} : -0.056$	$\lambda^{*OL}_{1T_2} : -0.363$
			$\lambda^{*OL}_{2T_1} : 2.497$	$\lambda^{*OL}_{2T_2} : 4.294$

The steady state comparisons in table 3 confirm the intuition that the FBNE will have higher regional temperatures and lower climate externality costs than both the cooperative solution and the OLNE. The case where the damages in region 1 from an increase in temperature in region 2 are higher than the corresponding damages in region 2, i.e. $d^l_{12} > d^l_{22}$, is of interest. This is because in this case there is a "flow" of damages from upstream to downstream and region 2 following feedbacks rules has strong incentives to increase its emissions and the temperature in region 2 since part of the damages will be realized in region 1. As indicated by the last row of table 3 the externality costate turns positive for region 2. This means that, since damages emerge in the South the benefits form increasing emissions in region 2, and therefore temperature, outweigh the damage cost from this temperature increase in region 2.

As in the case of OLNE a social planner seeking to implement the cooperative tax needs to impose an additional tax in each region. This additional tax should bridge the gap between the optimal tax under full cooperation and the regional FBNE value of the climate externality.

$$\tau_j^{*OPT} = -\lambda \left[\lambda^*_{T_1} + \lambda^*_{T_2}\right] - \left(-\lambda \left[V^{*FB}_{jT_1} + V^{*FB}_{jT_2}\right]\right), \text{ Region } j = 1, 2 \tag{33}$$

7. Two-Box Ramsey Type Models

This section develops a Ramsey-type modeling in the context of Alexeev and Jackson (2012), and Langen and Alexeev (2007) two-region climate models. We continue to make rather drastic simplifying assumptions in order to concentrate on the impact of heat transport.

In developing the Ramsey model, we explicitly consider a Cobb-Douglas production function in each region,

$$Y(x,t) = A(x,t)\, K(x,t)^{\alpha_K}\, L(x,t)^{\alpha_L}\, E(x,t)^{\alpha_E}\ ,\ x = 1, 2. \tag{34}$$

where $K(x,t)$ is the stock of capital and $A(x,t)$ is a productivity factor. Using this production function the capital budget constraint for each region becomes

$$\dot{K}(x,t) = Y(x,t) - C(x,t) - \delta K(x,t)\ ,\ x = 1, 2. \tag{35}$$

A deterministic Ramsey two-region optimization model is developed, which will be referred to as the "closed economy" problem. In this model each region is limited by its own budget constraint and no transfers between regions are taking place. The particular assumptions connected to this scenario are restrictive and perhaps not so realistic but they help to set up a benchmark model that can be compared with the other polar case in which the economy is completely open with free flows of capital, fossil fuel and consumption goods across locations.

Assuming that utility in each region is logarithmic in effective consumption $Ce^{-\phi(x,T_b+T)}$, the current value Hamiltonian for this Ramsey-type problem is:

$$\begin{aligned}
\mathcal{H} &= \sum_{x=1}^{x=2} \{ v(x) L(x,t) [\ln C(x,t) - \phi(x, T_b + T)] \\
&\quad -\lambda_{R_0^x}(t) E(x,t) \} + \\
&\quad \lambda_{T_1}(t) \frac{1}{H} [(-B - \gamma_1 - \gamma_2) T_1 + \gamma_1 T_2 + \\
&\quad \lambda [E(1,t) + E(2,t)]] + \\
&\quad \lambda_{T_2}(t) \frac{1}{H} [(\gamma_1 + \gamma_2) T_1 + (-B - \gamma_1) T_2 + \\
&\quad \lambda [E(1,t) + E(2,t)]] + \\
&\quad \sum_{x=1}^{x=2} \lambda_K(x,t) [Y(x,t) - C(x,t) - \delta K(x,t)] .
\end{aligned}$$

To be able to study steady states we make the simplifying assumptions of infinite reserves, so that $\lambda_{R_0^x}(0) = 0$, constant population and no productivity growth in each region so that $L(x,t) = L(x), A(x,t) = A(x)$. Under these simplifying assumptions, the optimality condition for the two-region Ramsey model can be written as follows. For the controls $C(x,t), E(x,t)$:

$$\begin{aligned}
\frac{v(x) L(x)}{C(x,t)} &= \lambda_K(x,t) \text{ or } C^0(x,t) = \frac{\alpha v(x) L(x)}{\lambda_K(x,t)} && (36) \\
(\lambda_{T_1}(t) + \lambda_{T_2}(t)) \frac{\lambda}{H} &= -\lambda_K(x,t) Z(x) \alpha_E K(x,t)^{\alpha_K} E(x,t)^{a_E - 1} \text{ or} && (37) \\
E^0(x,t) &= \left[\frac{-(\lambda_{T_1}(t) + \lambda_{T_2}(t)) (\lambda/H)}{\lambda_K(x,t) Z(x) \alpha_E K(x,t)^{\alpha_K}} \right]^{\frac{1}{a_E - 1}} && (38) \\
Z(x) &= A(x) L(x)^{\alpha_L} . && (39)
\end{aligned}$$

The complexity of the resulting Hamiltonian system does not allow analytical results. Therefore, some insight are obtained by resorting to simulations. For the climate system the parameters of the previous sections are used, while for the production system the following values are used.

$$\alpha_K = 0.35, a_L = 0.60, a_E = 0.05, A(1) = A(2) = 1, \delta = 0.05. \tag{40}$$

Steady-state results for the cooperative solution and the OLNE are shown below. All steady states have the saddle point property and the steady state externality tax is defined as $\tau = -\left(\lambda_{T_1} + \lambda_{T_2}\right) \frac{\lambda}{H}$,

Cooperative Solution: Steady states and Externality Tax (ET \$/tCO_2)

T_1	T_2	λ_{T_1}	λ_{T_2}	ET
0.95	1.66	-3.92	-5.52	52.51

OLNE: Steady states and Externality Tax (ET, \$/tCO_2) and Welfare Gain (WG) from moving to the cooperative solution

$(d_{12} < d_{22})$

T_1	T_2	λ_{1T_1}	λ_{1T_2}	λ_{2T_1}	λ_{2T_2}	ET_1	ET_2	WG_1	WG_2
1.63	2.85	-2.09	-2.69	-2.58	-3.95	26.54	36.32	16%	36.4%

$(d_{12} > d_{22})$

T_1	T_2	λ_{1T_1}	λ_{1T_2}	λ_{2T_1}	λ_{2T_2}	ET_1	ET_2	WG_1	WG_2
2.27	3.98	-3.86	-4.76	-1.11	-1.49	45.33	14.48	237%	47.3%

At the OLNE the additional tax in each region which is necessary to attain the cooperative steady state is ET-$ET_j, j = 1, 2$.

8. Conclusions

An important characteristic of climate feedbacks is the transfer of heat from the equator to the Poles. When extra forcing through anthropogenic emissions is present, this transfer creates Polar or Arctic amplification. PA in turns could induce a "flow of damages" from the Poles to the South. In the present paper, a two-box, or two-region climate model, which allows for heat and moisture transport from the southern region to the northern region is coupled with an economic model of welfare optimization.

In the economic model, fossil fuel use or emissions are determined at cooperative and noncooperative solutions. Non-cooperative solutions correspond to open loop and feedback Nash equilibrium solutions for the two regions. Non-cooperative solutions are asymmetric. Asymmetries stem from the differentiation of damages in each region due to PA.

Using numerical simulations it is shown, in line with previous findings, that ignoring spatial heat and moisture transport and the resulting PA, results in welfare loss and bias in a tax on GHG emissions. The results hold both for cooperative and non-cooperative solutions. The effects are however asymmetric and depend on which region suffers higher damages from PA.

When damages from PA are higher in region 1 than region 2, results suggest that at a non-cooperative solution region 2 has an incentive to increase emissions, especially when feedback strategies are followed, since a part of these damages move "downstream" to region 1.

The asymmetric behavior of regions at the non-cooperative solutions suggest that when each region follows a climate policy maximizing its own welfare, then different additions to regional carbon taxes should be applied if the objective is to attain the cooperative paths for emissions and temperature anomalies. The results remain robust when the model is extended to cooperative and OLNE solutions of a Ramsey type growth model with heat transfer and PA.

Regarding the numerical estimates which provide the main quantitative insights, the present model – like many stylized abstract models – is meant only to be suggestive of what a more realistic exercise might find. Complex models, like most of the IAMs, are difficult to comprehend, especially regarding the emergence of the numerical results (van der Ploeg and Rezai, 2016). On the other hand, relatively simple models could provide a framework where the theoretical predictions seem to be confirmed by the numerical exercises.

The present model could be extended along different lines. The spatial structure could be enhanced by allowing for more regions, stochastic shocks could be introduced, and more advanced computational methods could be applied to solve the nonlinear feedback problem instead of using its linear-quadratic approximation. One of the most important issues, however in this type of spatial modeling is the adequate estimation of regional damages. This is a crucial area for further research which will provide credibility to the quantitative estimates obtained from the models. For example if heat transfer from Equator to Poles did not exist damages from extreme heat documented by Hsiang et al (2017) in the low latitudes may be even larger and mortalities from both extreme heat in the low latitudes and extreme cold in the high latitudes documented by Gasparrini et al (2015) may be even larger. Detailed work on estimating marginal temperature and damage impacts due to Equator to Pole heat transport will be needed in order to compute its impact on optimal policy.

Another important area of future research is to exploit recent work on emulation of responses of Atmospheric Ocean General Circulation Models (AOGCMs) in order to improve modeling of the climate dynamics component of our model.

E.g. Castruccio et al. (2014) fit the equation

$$
\begin{aligned}
T_t &= \beta_0 + \beta_1 \frac{1}{2}\left[\ln \frac{CO_{2,t}}{CO_{2,0}} + \ln \frac{CO_{2,t-1}}{CO_{2,0}}\right] + \beta_2 (1-\rho) \sum_{k=2}^{k=t} \rho^k \ln \frac{CO_{2,t-k}}{CO_{2,0}} + \varepsilon_t \\
\varepsilon_t &= \phi \varepsilon_{t-1} + \sigma z_t \ , \ \ \{z_t\} \ IIDN(0,1) \\
& \quad T_0 \text{ given, } CO_{2,t} \text{ concentration of } CO_2 \text{ at } t, \ CO_{2,0} \text{ preindustrial concentration,}
\end{aligned}
$$

to regional yearly temperature data generated by their AOGCM for one scenario to "train" their emulator. They then use their estimated equation for that scenario to mimic the output of their AOGCM for another scenario. They do this procedure for 47 regions (See Table S1 of Castruccio et al (2014) SOM for estimates). Their performance measure suggests that the emulator does a fairly good job of mimicking the output of the much more complicated AOGCM. Castruccio et al. (2014, Figure 6) displays the emulated temperatures with the top of the display corresponding to northern latitude regions and the southern latitude regions at the bottom. The pattern of higher temperatures as one moves towards the northern regions is clear.

The advantage of emulation rather than our use of the Matthews et al (2009) and Leduc et al. (2016) approximate relationship between cumulative emissions and temperature change is that climate scientists argue that it is more appropriate to longer time scales than yearly whereas yearly time scales are more appropriate for economic analysis. Brock and Xepapadeas (2017) exhibited a plot at time scales appropriate to economic using MacDougall and Friedlingstein's (2015) equations that lie behind the Matthews et al (2009) approximation of temperature response to cumulative emissions. While their plot was approximately linear at the yearly time scale which supports using the Matthews et al (2009) approximation at the yearly time scale, future research should use better approximations of temperature response to cumulative emissions at the yearly time scale. Future research should use the work on emulators to get a better model of climate dynamics in our model.

References

[1] Alexeev, V.A., Jackson, C.H., 2012. Polar amplification: is atmospheric heat transport important? Climate Dynamics, DOI 10.1007/s00382-012-1601-z.

[2] Alexeev, V.A., Langen, P.L., Bates, J.R., 2005. Polar amplification of surface warming on an aquaplanet in "ghost forcing" experiments without sea ice feedbacks. Climate Dynamics, DOI 10.1007/s00382-005-0018-3.

[3] Başar, T., Geert Jan Olsder, G.J., 1995. Dynamic noncooperative game theory. London: Academic Press.

[4] Bekryaev, R., Polyakov, I., Alexeev, V., 2010. Role of polar amplification in long-term surface air temperature variations and modern arctic warming. Journal of Climate 23, 3888-3906.

[5] Brock, W., Engström, G., Xepapadeas, A., 2014. Energy balance climate models, damage reservoirs, and the time profile of climate change policy. In: Bernard, L., Semmler, W. (Eds), The Oxford Handbook of the Macroeconomics of Global Warming. Oxford University Press, Oxford, chapter 3.

[6] Brock, W., Engström, G., Xepapadeas, A., 2014a. Spatial climate-economic models in the design of optimal climate Policies across Locations, European Economic Review, 69, 78-103.

[7] Brock, W., Xepapadeas, A., 2017. Climate change policy under polar amplification. European Economic Review 94, 263–282. DOI: http://dx.doi.org/10.1016/j.euroecorev.2017.03.003.

[8] Brock, W., Xepapadeas, A., 2017a. Spatial Heat Transport, Polar Amplification and Climate Change Policy, in G. Chichilnisky and A. Rezai (Eds), Handbook of Climate Change, Oxford University Press, forthcoming

[9] Cai, Y. Brock, W., and A. Xepapadeas, 2017. Climate Change Economics and Heat Transport across the Globe: Spatial-DSICE, ASSA annual meeting Chicago, http://purl.umn.edu/251833.

[10] Castruccio, S., Mcinerney, D., l. Stein, M., Crouch, F., Jacob, R., Moyer, E., 2014, Statistical emulation of climate model projections based on precomputed GCM Runs, Journal of Climate Science, 27, 1829-1844.

[11] Dietz, S., Stern, N., 2015. Endogenous growth, convexity of damage and climate risk: how Nordhaus' framework supports deep cuts in carbon emissions. The Economic Journal 125 (583), 547-620.

[12] Francis, J., Skific, N., 2015. Evidence linking rapid Arctic warming to mid-latitude weather patterns. Philosophical Transactions of the Royal Society A 373, dx.doi.org/10.1098/rsta.2014.0170.

[13] Francis, J., 2017. Why Are Arctic Linkages to Extreme Weather Still Up in the Air?, forthcoming BAMS 21, 221–232.

[14] Gasparrini, A., Yuming Guo, Masahiro Hashizume, Eric Lavigne, Antonella Zanobetti, Joel Schwartz, Aurelio Tobias, Shilu Tong, Joacim Rocklöv, Bertil Forsberg, Michela Leone, Manuela De Sario, Michelle L Bell, Yue-Liang Leon Guo, Chang-fu Wu, Haidong Kan, Seung-Muk Yi, Micheline de Sousa Zanotti Stagliorio Coelho, Paulo Hilario Nascimento Saldiva, Yasushi Honda, Ho Kim, Ben Armstrong, 2015, Mortality risk attributable to high and low ambient temperature: a multicountry observational study, www.thelancet.com, Published online May 21, 2015 http://dx.doi.org/10.1016/S0140-6736(14)62114-0.

[15] Hsiang, S., Robert Kopp, Amir Jina, James Rising, Michael Delgado, Shashank Mohan, D. J. Rasmussen, Robert Muir-Wood, Paul Wilson, Michael Oppenheimer, Kate Larsen, Trevor Houser, (2017), Estimating economic damage from climate change in the United States, Science 356, 1362–1369.

[16] IPCC, 2013. Climate Change 2013, The Physical, Science Basis. Cambridge University Press, New York.

[17] Langen P.L., Alexeev, V.A., 2007. Polar amplification as a preferred response in an idealized aquaplanet GCM. Climate Dynamics, DOI 10.1007/s00382-006-0221-x.N/EE-0564-112.pdf/$file/EE-0564-112.pdf.

[18] Lenton, T., Held, H., Kriegler, E., Hall, J., Lucht, W., Rahmstorf, S., Schellnhuber, H.J., 2008. Tipping elements in the Earth's climate system. PNAS 105(6), 1786-1793.

[19] Leduc, M., H. Damon Matthews, and Ramón de Elía, 2016, Regional estimates of the transient climate response to cumulative CO2 emissions, Nature Climate Change.

[20] MacDougal, A.H, Friedlingstein, P., 2015. The origin and limits of the near proportionality between climate warming and cumulative CO2 emissions. Journal of Climate 28, 4217-4230.

[21] Matthews, H.D., Gillett, N.P., Stott, P.A., Zickfield, K., 2009. The proportionality of global warming to cumulative carbon emissions. Nature 459, 829-833.

[22] North, G.R., 1975a, Analytical solution to a simple climate model with diffusive heat transport, Journal of the Atmospheric Sciences 32:1301-1307.

[23] North, G.R., 1975b, Theory of energy-balance climate models, Journal of the Atmospheric Sciences 32:2033-2043.

[24] North, G. R., Cahalan, and J. Coakely, 1981, Energy balance climate models, Reviews of Geophysics and Space Physics 19(1): 91-121.

[25] van der Ploeg, F., Rezai, A., 2016. Cumulative emissions, unburnable fossil fuel, and the optimal carbon tax. Technolg. Forecas. Soc. Change, http://dx.doi.org/10.106/j.techfore.2016.10.016.

[26] Whiteman, G., Chris Hope & Peter Wadhams, 2013, Climate science: Vast costs of Arctic change Nature 499, 401–403 doi:10.1038/499401a

[27] Wu, W. and G.R. North, 2007, Thermal decay modes of a 2-D energy balance climate model, Tellus A 59(5): 618–26.